EUROPEAN ORGANIZATION FOR NUCLEAR RESEARCH
Laboratory for Particle Physics

Departmental Report

CERN/AT 2006-2 (MAS)

INTRODUCTION OF REFERENCE DESIGN 2 FOR THE NED 15 T LARGE APERTURE DIPOLE

N. Schwerg[1], A. Devred[1,2], C. Vollinger[1]

In this report, the results of the electromagnetic design study for the cos θ-layer-type dipole are presented. The final configuration is referred to as Reference Design 2 for NED. The studied dipole is an 88 mm large bore, single aperture dipole surrounded by an iron yoke. It relies on the specifications for the Nb_3Sn strand and the Rutherford-type cable as well as on the material properties, the agreed dimensions and the maximum forces agreed upon by the collaboration. This design study is in the framework of CERN contributions to NED.

1 CERN, Accelerator Technology Department, Geneva, Switzerland
2 CEA/DSM/DAPNIA/SACM, Saclay, France

Administrative Secretariat
AT Department
CERN
CH - 1211 Geneva 23

Geneva, Switzerland
10 May 2006

1 Introduction

In the framework of research and development (R&D) activities at CERN, the Next European Dipole (NED) program is dedicated to the development of a high-field dipole magnet using Nb_3Sn superconductors. Part of the NED activities which are shared amongst several collaborating institutes [1], is a design study of different possible dipole configurations able to reach 15 T at quench.

In this note, the results of the electromagnetic design study for the $\cos\theta$-layer-type dipole [2] are presented. The final configuration is referred to as Reference Design 2 for NED. The studied dipole is an 88 mm large bore, single aperture dipole surrounded by an iron yoke. It relies on the specifications for the Nb_3Sn strand [1], the Rutherford-type cable [3], as well as on the material properties [4, 5], the dimensions [6] and the maximum forces [7] agreed upon by the collaboration.

All calculations are carried out by means of the CERN field computation program **ROXIE** [5]. The simulation of persistent current induced field errors is carried out by means of the intersecting-ellipse model [8] based on the estimation of the critical current density presented in [9].

Starting from the Reference Design 1 [3], the coil cross section was optimized with respect to field quality and conductor alignment. The shape of the iron yoke was optimized in order to minimize the influence of the iron saturation on the relative multipole errors during ramp up and an improvement of the geometric multipole coefficients could be reached. In addition, a suitable way for the compensation of persistent current induced field errors is presented.

2 Reference Design 2: Coil Cross Section and Iron Yoke Design

For the compensation of iron saturation effects, an iron yoke with an elliptical inner contour is used. This allows in a relatively simple way a steering of the field variation during ramp up especially for multipoles b_3 and b_5, with only small losses in main field strength. The final iron geometry is shown in fig. 1 and the used values are given in tab. 1. Note that from the mechanical point of view, the punching of the ellipse as well as the force transmission between iron yoke and collar have to be further investigated.

The corresponding design of the coil cross section is shown in fig. 2 while the electromagnetic properties and the performance of Reference Design 2 are summarized in tab. 2 such that it is comparable to the different designs and a selection of the most suitable cross-section for the NED dipole can take place. Since there is only a small keystoning foreseen in the cable cross section, the design of the large aperture dipole for NED has to satisfy stringent requirements to the conductor placements. Therefore, a large effort has been denoted in the design process to align the conductors in a radial position around the winding post in order to avoid that too much stress is applied on the cable. As a consequence, all conductor blocks are radially aligned, with the exception of block 5.

The calculated multipole errors at high field (8.5% margin on the load line) are shown in tab. 3 and the curves showing the variation of the multipole errors versus excitation current (without considering superconductor magnetization effects) are shown in fig. 3. The values of the total variation of the lower-order multipole coefficient from low to high field are given in tab. 4. In order to judge the numbers and to show that the design qualifies as an accelerator-class magnet, the obtained multipole values are compared to the target values of LHC in table 6. The numbers have been re-scaled from the NED reference radius to the LHC reference radius[1] of 17 mm.

Table 1: Salient specified radii and semi-axes for the 88 mm NED magnet.

Quantity	Value	Unit
Reference radius r_0	29	mm
Aperture radius r_A	44	mm
Inner radius of outer layer r_{L2}	73	mm
Inner collar radius r_{Ci}	100.4	mm
Outer collar radius r_{Co}	125.4	mm
Inner yoke semi minor axis (at x-axis) b_{Yi}	125.4	mm
Inner yoke semi major axis (at y-axis) a_{Yi}	138.6	mm
Outer yoke radius r_{Yo}	475.4	mm

The persistent current induced field errors for Reference Design 2 without any additional compensation measures are shown (for comparison of b_3 and b_5) in fig. 4. After a pre-cycle, the powering current is ramped up from low values (approximately 5% of the maximum current) to maximum current (at a margin on the load line of 8.5%) and again down to low current. All multipole errors show a hysteresis. The loops are following different orientations, going counter-clockwise for b_3 and b_7 and clockwise for b_5 and b_9. All loops show a spike where the ramp direction is changed and a relative extreme value at approximately 3 kA on the up ramp branch. The hysteresis width strongly decreases with increasing excitation current. The values at the operation point are close to the optimized values shown in tab. 3. The strongest variation is between the spike at low excitation and the relative extreme value. Table 5 shows the variation of the relative multipole errors Δb_n between the relative extreme value and the value at maximum current.

[1] We used the multipole scaling law for radii: $b_n(r_1) = (r_1/r_0)^{n-N} b_n(r_0)$, where $N = 1$ for a dipole geometry.

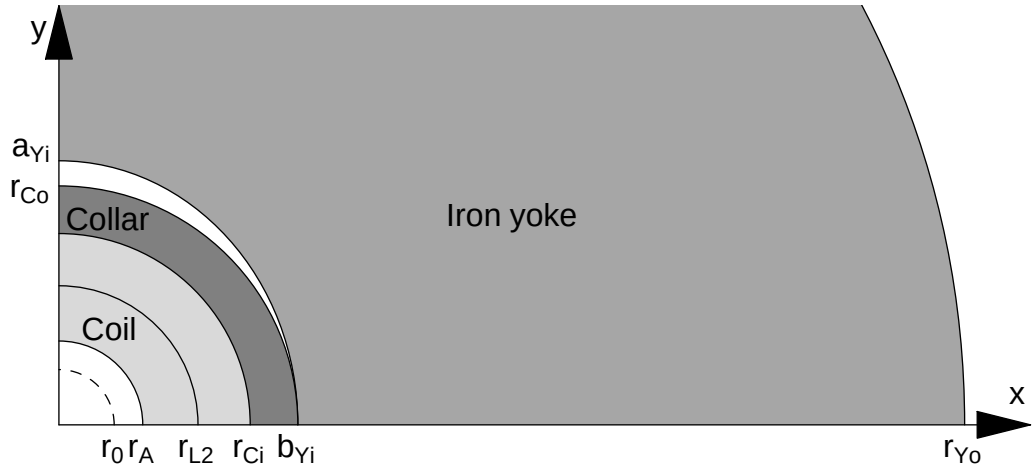

Figure 1: Sketch of magnet cross section with stainless steel collar and iron yoke defining the most salient radii and semi axes.

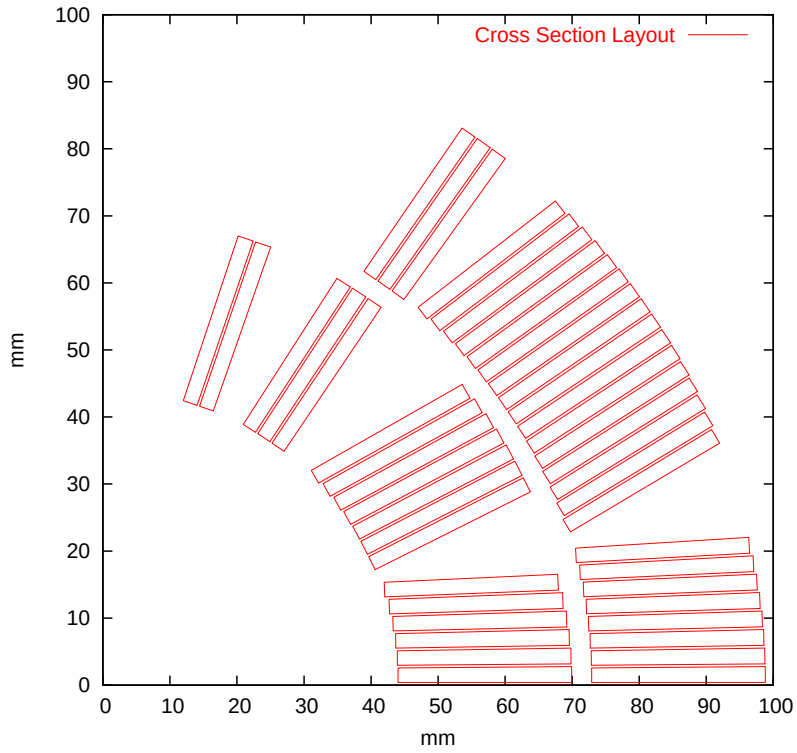

Figure 2: Optimized coil cross section (to be used with an elliptical iron yoke).

Table 2: Salient electromagnetic properties of Reference Design 2 (at a margin on the load line of 8.5%).

Quantity	Value	Unit
Excitation current	26670	A
Main field B_1	−13.31	T
Peak field on conductor B_{peak}	13.75	T
Peak field / main field	1.032	-
Stored magnetic energy per unit length	1.556	MJ/m
Inductance per unit length	4.375	mH/m
Horizontal force F_x per side and per unit length	13.79	MN/m
Stress on the midplane (inner layer)	−118.7	MPa
Stress on the midplane (outer layer)	−131.8	MPa
Excitation current at 0% margin on the load line	29440	A
Peak field at 0% margin on the load line	15.00	T

Table 3: Relative multipole errors b_n in units given at a reference radius of 29 mm for Reference Design 2 (at a margin on the load line of 8.5%).

b_3	b_5	b_7	b_9	b_{11}	b_{13}	b_{15}
−0.018	0.058	0.077	1.703	2.692	−0.046	−0.176

Table 4: Variations of the multipole coefficients Δb_n induced by the iron yoke saturation during a current ramp from 1.3 kA to ≈ 27 kA.

Δb_3	Δb_5	Δb_7	Δb_9
5.35	0.51	0.018	0.12

Table 5: Variations of the multipole coefficients induced by superconductor magnetization currents on the up ramp branch. The variation from the extreme value at around 3 kA to the extreme value close to the maximum current value is given.

Δb_3	Δb_5	Δb_7	Δb_9
40	9.5	2.2	2.4

Table 6: Comparison of NED multipole errors given in units with target values for LHC. The NED values have been re-scaled to the LHC reference radius of 17 mm.

b_3	b_5	b_7	b_9	b_{11}	b_{13}	b_{15}	
−0.01	0.017	0.013	0.152	0.131	0.001	0.003	NED at 17 mm
1.33	−0.3	0.32	0.13	0.53	–	–	LHC target at 17 mm

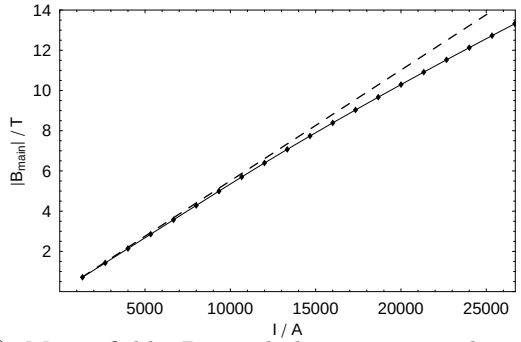

(a) Main field B_1 and linear extrapolation (dashed) versus excitation current.

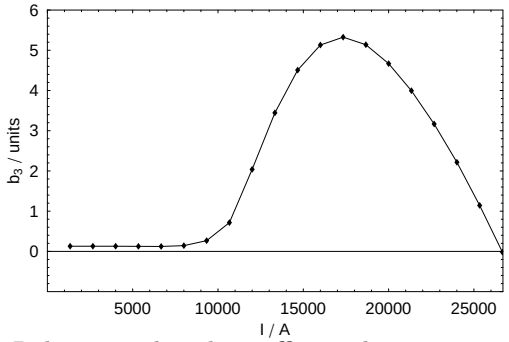

(b) Relative multipole coefficient b_3 versus excitation current.

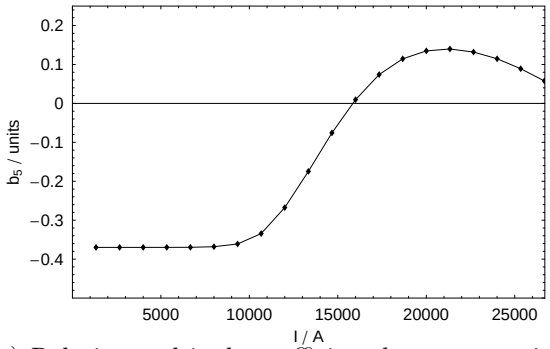

(c) Relative multipole coefficient b_5 versus excitation current.

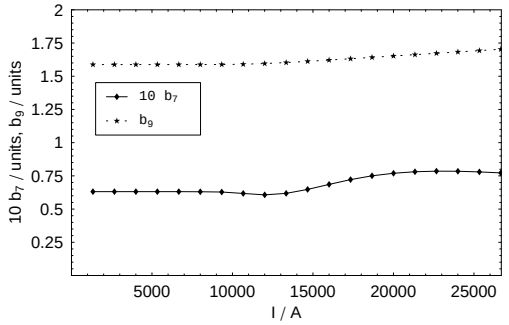

(d) Relative multipole coefficients 10 b_7 and b_9 versus excitation current.

Figure 3: Variation of the main field and the lower order multipole coefficients with increasing powering current for Reference Design 2 taking into consideration the effect of iron saturation.

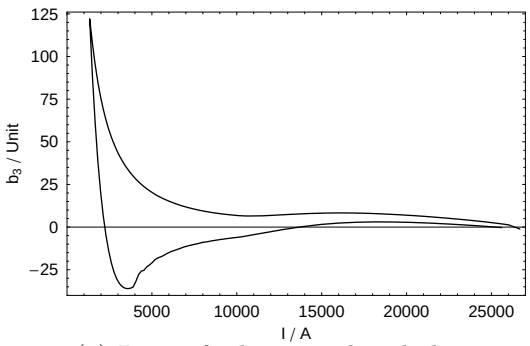

(a) Loop of relative multipole b_3

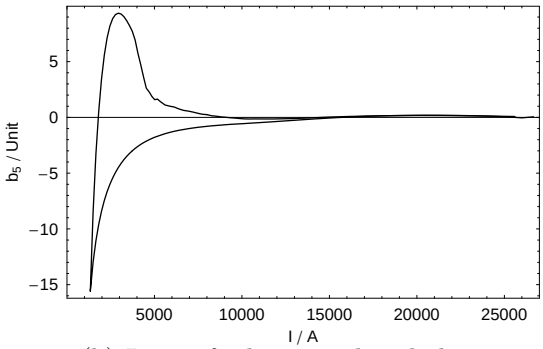

(b) Loop of relative multipole b_5

Figure 4: Variation of the multipole coefficients induced by superconductor magnetization currents for Reference Design 2 (without any compensation by means of ferromagnetic shims). The current ramp cycle is from $\approx 1.5\,\mathrm{kA}$ up to $\approx 27\,\mathrm{kA}$ and down to $\approx 1.5\,\mathrm{kA}$.

3 Additional Compensation of Persistent Current Induced Field Errors

In [3], the compensation of persistent current induced field errors was studied by means of ferromagnetic wedges replacing the non magnetic copper wedges. The study showed a very strong effect on b_3, much stronger than needed for the compensation. By reducing the size of the ferromagnetic part of the wedge, the saturation starts earlier and the overall effect can be reduced. For the design presented here, this is done by shims on one of the broad surfaces of the wedge.

The ideal positions for the ferromagnetic shims can be found by means of analytical estimations [2] and the final shim thickness can be determined by means of numerical optimizations. The presented compensation relies on two shims, each of 26.4 mm width but different thicknesses, one placed in the inner and one in the outer layer (as shown in fig. 5). The shim in the inner layer situated on top of block 5 is 0.702 mm thick whereas the shim in the outer layer on top of block 2 is of 1.5 mm thickness.

In order to demonstrate how the compensation method works on the different multipole coefficients, figure 6 shows the influence of the two shims on the field errors induced only by the coil geometry and the iron yoke saturation.

Figure 7 shows the simulated multipole errors including the calculation of persistent current induced field errors for the compensation with the two specified shims.

It can be seen that the variation of b_3 is strongly reduced. Also, the variation of b_5 is decreased and even slightly over compensated. As could be expected from fig. 6, the variations of b_7 and b_9 have been amplified. Table 7 shows the calculated variation of the relative multipole errors.

4 Summary

The proposed NED Reference Design 2 could be re-optimized to improved geometric multipole coefficients. Its conductor blocks assume close to radial positions and its elliptical yoke enables a significant reduction of the saturation effects. Furthermore, we have outlined a simple and effective method to compensate the persistent magnetization current effects.

The next step will be to work on the mechanical design and to use the results of this study for the next iteration.

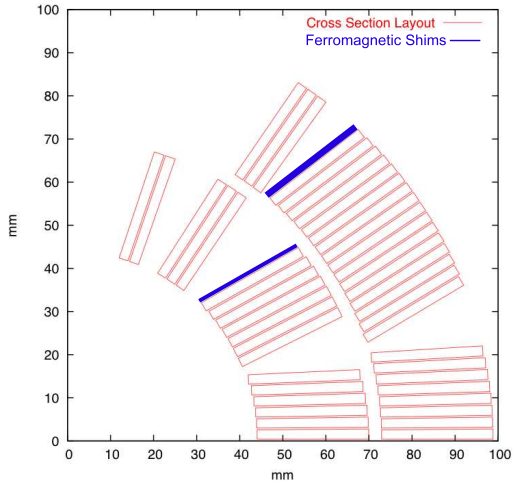

Figure 5: Coil cross section of Reference Design 2 including two ferromagnetic shims for the compensation of persistent current induced field errors.

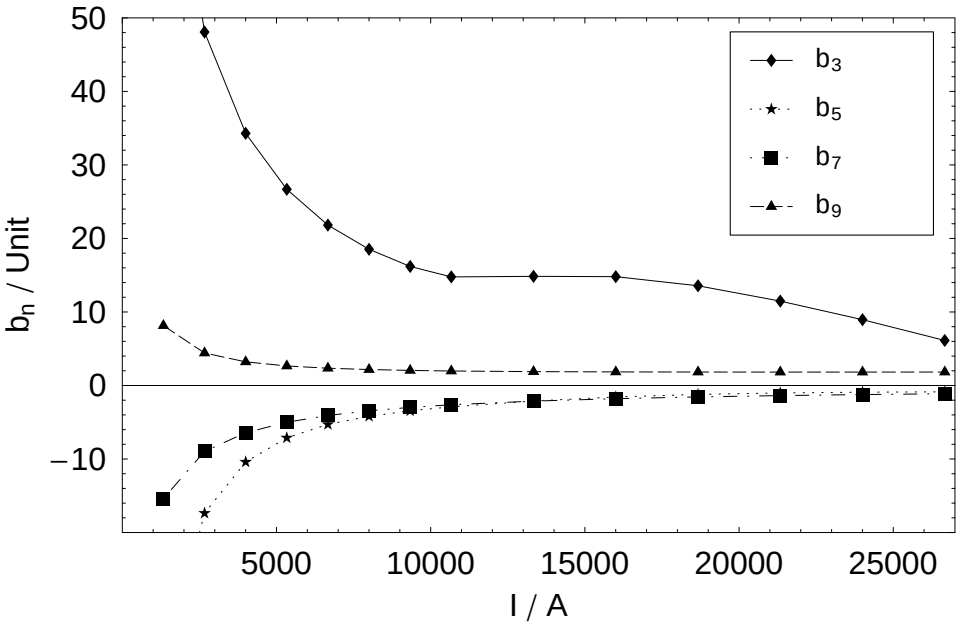

Figure 6: Variation of the lower order relative multipole coefficients (at a reference radius of 29 mm) due to the iron saturation for the final coil cross section with elliptical iron yoke and one ferromagnetic shim on top of block 2 and one on top of block 5. The shims have a width of 26.4 mm and a thickness of 1.5 mm for the outer layer and 0.702 mm for the inner layer.

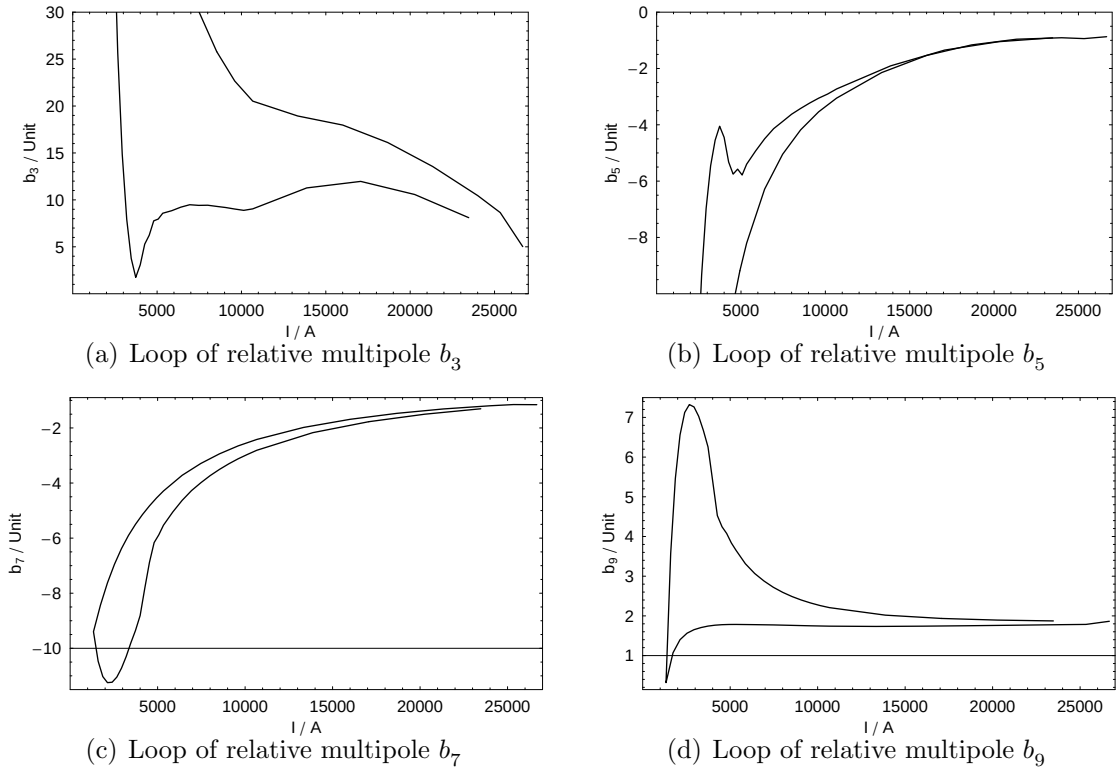

(a) Loop of relative multipole b_3

(b) Loop of relative multipole b_5

(c) Loop of relative multipole b_7

(d) Loop of relative multipole b_9

Figure 7: Field errors (at a reference radius of 29 mm) induced by superconductor magnetization for Reference Design 2 after insertion of ferromagnetic shims. The current ramp cycle is from ≈ 1.5 kA up to ≈ 27 kA and down to ≈ 1.5 kA. The variation of b_3 and b_5 on the up ramp branch above ≈ 4 kA have been strongly reduced. The cross section has not been reoptimized after shim insertion.

Table 7: Variation of multipole coefficients induced by superconductor magnetization currents on the up ramp branch. The variation from the extreme value at around 4 kA to the extreme value close to the maximum current value is given.

Δb_3	Δb_5	Δb_7	Δb_9
10	5	10	7.4

References

[1] A. Devred, *et al.*, "Status of the Next European Dipole (NED) Activity of the Collaborated Accelerator Research in Europe (CARE) Project," in *Transactions on Applied Superconductivity*, vol. 15, no. 2, June 2005, pp. 1106–1112.

[2] N. Schwerg, "Electromagnetic design study for a large bore 15t superconducting dipole magnet," Diplomarbeit, Technische Universität Berlin, Berlin, Germany, nov 2005. [Online]. Available: http://cdsweb.cern.ch/search.py?recid=914515&ln=en

[3] D. Leroy and O. Vincent-Viry, "Preliminary Magnetic Designs for Large-Bore and High-Field Dipole Magnets," CERN, Geneva, Switzerland, Tech. Rep., Dec. 2004.

[4] P. Loverige, "Thermal Contraction Factors for NED," Private communciation, RAL, Oxford, Great Britain, Apr. 2005.

[5] S. Russenschuck, *Electromagnetic Design and Optimization of Accelerator Magnets*, 2nd ed. Geneva, Switzerland: CERN, June 2005, ISBN: 92-9083-242-8.

[6] A. Devred, P. Loveridge, and N. Schwerg, "Yoke Radii for NED," Private communication, June 2005.

[7] P. Fessia, "Stress and forces in the coil cross section of superconducting magnets," Private communication, CERN, Geneva, Switzerland, Mar. 2005.

[8] C. Völlinger, "Superconductor Magnetization Modeling for the Numerical Calculation of Field Errors in Accelerator Magnets," Ph.D. dissertation, Technische Universität Berlin, CERN, Switzerland, oct 2002.

[9] N. Schwerg, A. Devred, and C. Völlinger, "Estimation of the Critical Current Density for the Strand Used for NED," Technical Note, CERN, Geneva, Switzerland, Sept. 2005, to be published.